

# Critical-state effects on microwave losses in type-II superconductors

M. Bonura, E. Di Gennaro, A. Agliolo Gallitto, and M. Li Vigni  
*CNISM and Dipartimento di Scienze Fisiche ed Astronomiche,  
 Università di Palermo, Via Archirafi 36, I-90123 Palermo, Italy*

(Dated: December 2, 2024)

We discuss the microwave energy losses in superconductors in the critical state. The field-induced variations of the surface resistance are determined, in the framework of the Coffey and Clem model, by taking into account the distribution of the vortex magnetic field inside the sample. It is shown that the effects of the critical state cannot generally be disregarded to account for the experimental data. Results obtained in bulk niobium at low temperatures are quantitatively justified.

PACS numbers: 74.25.Ha, 74.25.Op, 74.25.Nf

Investigation of fluxon dynamics in type-II superconductors is of great interest for both fundamental and applicative aspects. From the basic point of view, it allows measuring the relative magnitude of elastic and viscous forces, which rule the motion regime of the fluxon lattice [1, 2, 3, 4]. From the technological point of view, it allows determining the critical current, accounting for the energy losses and investigating the presence of irreversible phenomena, which are important factors for the implementation of superconductor-based devices.

A suitable method to investigate the fluxon dynamics consists in determining the field-induced energy losses at microwave (mw) frequencies, by measuring the surface resistance,  $R_s$  [2]. In the absence of static magnetic fields, the variation with the temperature of the condensed-fluid density determines the temperature dependence of  $R_s$ . On the other hand, the field dependence of  $R_s$  in superconductors in the mixed state is determined from the presence of fluxons, which bring about normal fluid in their cores, as well as the fluxon motion [1, 2, 3, 4, 5, 6, 7].

Coffey and Clem (CC) have elaborated a comprehensive theory for the electromagnetic response of type-II superconductors in the mixed state [5], taking into account flux creep, flux flow, and pinning effects in the framework of the two-fluid model. The theory has been developed with two basic assumptions: i) inter-vortex spacing much less than the field penetration depth; ii) uniform vortex distribution in the sample. With these assumptions, the local vortex magnetic field,  $B(\mathbf{r})$ , averaged over distances larger than several inter-vortex spacings, is spatially uniform. As pointed out by the authors [5], the first assumption is valid when the external field,  $H_0$ , is greater than  $2H_{c1}$ ; whereas, the second one does not take into account the magnetic history of the sample.

When the external magnetic field develops a critical state of the vortex lattice [8, 9], the assumption that  $B$  is uniform is not longer valid. In this case, the CC model does not account for the experimental results; for instance, no magnetic hysteresis in the  $R_s(H_0)$  curves is expected. Though different authors have justified the hysteretic behavior of the  $R_s(H_0)$  curves by considering critical-state effects in the fluxon lattice [10, 11], the field

dependence of the surface resistance for non-uniform flux profile has never been quantitatively investigated.

In this letter we give a generalization of the CC theory, taking into account the flux distribution inside the sample, due to the critical state. We will show that the  $R_s(H_0)$  curve strongly depends on the specific profile of the magnetic induction  $B$ , determined by the field dependence of the critical current density  $J_c(B)$ . We will report experimental results of the field-induced variations of  $R_s$  in a niobium bulk sample in the critical state; the results are quite well accounted for by considering a specific  $B$  profile inside the sample.

In the London local limit, the surface impedance is proportional to the complex penetration depth  $\tilde{\lambda}$  of the em field. In particular,

$$R_s = -\mu_0 \omega \operatorname{Im}[\tilde{\lambda}(\omega, B, T)]. \quad (1)$$

In the CC model,  $\tilde{\lambda}(\omega, B, T)$  is given by

$$\tilde{\lambda}(\omega, B, T) = \sqrt{\frac{\lambda^2(B, T) + (i/2)\tilde{\delta}_v^2(\omega, B, T)}{1 - 2i\lambda^2(B, T)/\delta_{nf}^2(\omega, B, T)}}, \quad (2)$$

with

$$\lambda(B, T) = \frac{\lambda_0}{\sqrt{[1 - (T/T_c)^4][1 - B/B_{c2}(T)]}}, \quad (3)$$

$$\delta_{nf}(\omega, B, T) = \frac{\delta_0}{\sqrt{1 - [1 - (T/T_c)^4][1 - B/B_{c2}(T)]}}, \quad (4)$$

where  $\lambda_0$  is the London penetration depth at  $T = 0$  and  $\delta_0$  is the normal-fluid skin depth at  $T = T_c$ .

$\tilde{\delta}_v$  is the effective complex skin depth arising from the vortex motion; it depends on the relative magnitude of the viscous and restoring pinning forces. In the following, we will devote the attention to the case in which the vortex lattice moves in the flux-flow regime, where the fluxon motion is ruled by the viscous force; in this case, considering the expression of the viscous coefficient proposed by Bardeen and Stephen [12], it results  $\tilde{\delta}_v^2 = \delta_0^2 B/B_{c2}(T)$ . The real part of  $\tilde{\lambda}$  defines the ac penetration depth,  $\lambda_{ac}$ .

Since the mw losses depend on the local magnetic field  $B(\mathbf{r})$ , when it is not uniform, different regions of the sample contribute to the energy losses differently; this should occur when the sample is in the critical state. Generally, the critical state develops at temperatures smaller enough than  $T_c$ , where the pinning effects are significant; in this case, the energy losses are mainly related to the motion of fluxons induced by the mw current. So, a discriminating criterium to determine in what extent the non-uniform  $B$  profile affects the energy losses consists in evaluating the magnetic-field variation in the region where fluxons feel the Lorentz force. For the sake of clearness, we limit the analysis to a slab geometry (sample width  $w$ , with  $w \gg \lambda_{ac}$ , and height  $d$ ). We suppose that the static magnetic field,  $H_0$ , is greater than  $H_{c1}$  and that the sample is in a critical state à la Bean, i.e. characterized by a field-independent  $J_c$  [8]; however, the analysis applies to any  $J_c(B)$  dependence.

Fig. 1 describes the distribution of the fields and the mw current in the two geometries:  $\mathbf{H}_\omega \parallel \mathbf{H}_0$  (a);  $\mathbf{H}_\omega \perp \mathbf{H}_0$  (b). When the mw magnetic field is parallel to the  $z$ -axis, the mw current penetrates in the surface layers of the sample, of width  $\lambda_{ac}$ , in the  $x - y$  plane. If  $\mathbf{H}_\omega \parallel \mathbf{H}_0$ , only the fluxons in these layers experience the Lorentz force, due to the mw current, and the fluxon lattice undergoes a compressional motion. In Fig. 1 (a) we analyze the regions indicated by the shadowed area. In this case, if the variation of  $B$  in these regions is negligible, i.e.  $J_c \lambda_{ac} \ll H_0$ , the vortex magnetic field can be considered as uniform. A different situation occurs when  $\mathbf{H}_\omega \perp \mathbf{H}_0$ , as shown in Fig. 1 (b); in this case, all the vortices present in the sample are involved in the motion, the fluxon lattice undergoes a tilt motion [6],  $\lambda_{ac}$  determines the part of the flux line in which the Lorentz force acts; the approximation of  $B$  uniform would be proper only if the sample width is such that  $J_c w \ll H_0$ . So, for bulk samples, it is expected that the specific profile of  $B$  strongly affects the  $R_s(H_0)$  curve; indeed, different regions of the sample contribute in different extent to the mw energy losses. In the following, we will refer to this field geometry, where the effects of the non-uniform profile of  $B$  most affect the  $R_s(H_0)$  curve.

Brandt [6] has shown that the compressional and tilt motion of the fluxon lattice can be described by the same formalism and, in particular for weak pinning, the same ac penetration depth results because the compression and tilt moduli are approximately equal. So, the results obtained from the CC model are valid even in the case of tilt motion provided that  $B$  is uniform in the region where the Lorentz force is active.

When the sample is in the critical state, one can subdivide its surface in different regions, in each of them  $B(\mathbf{r})$  can be considered uniform. Each part of the surface is characterized by a different  $R_s$  value, due to the local magnetic induction, and the energy losses of the whole sample are determined by the surface-resistance contribu-

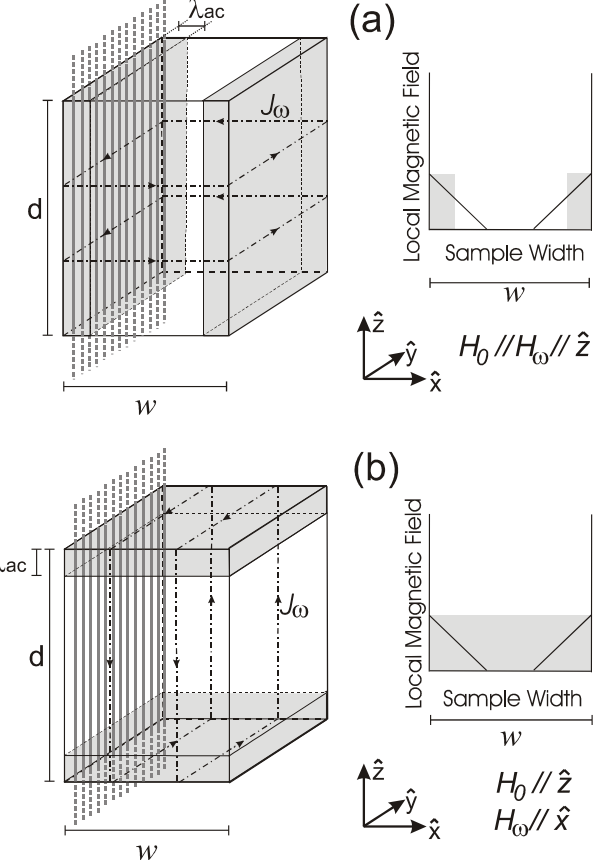


FIG. 1: Distribution of the fields and current in two different geometries:  $\mathbf{H}_\omega \parallel \mathbf{H}_0$  (a);  $\mathbf{H}_\omega \perp \mathbf{H}_0$  (b); the shadowed area indicates the regions of the sample interested by the vortex motion.

butions of each region. The measured surface resistance is an averaged value over the whole sample:

$$R_s = \frac{1}{S} \int_{\Sigma} R_s(|B(\mathbf{r})|) dS, \quad (5)$$

where  $\Sigma$  is the sample surface,  $S$  is its area and  $\mathbf{r}$  identifies the surface element; the main contribution comes from the sample regions where  $\mathbf{H}_0 \times \mathbf{J}_\omega \neq 0$ .

In the flux-flow regime, in order to calculate the surface resistance, normalized to the normal-state value at  $T = T_c$ ,  $R_n$ , using Eqs. (1–4), it is necessary to know the ratio  $\lambda_0/\delta_0$  and the upper critical field [13]. Moreover, to take into account the critical-state effects, by Eq. (5), it is also necessary to know the  $B$  profile inside the sample, determined by  $J_c(B)$ . Fig. 2 shows  $R_s/R_n$  as a function of the reduced field,  $H_0/H_{c2}$ , in three different cases. Curve (a) is the one expected from the CC model ( $J_c = 0$ ). Curves (b) and (c) have been obtained with  $J_c = J_{c0}$ , independent of  $B$ , and two different values of the full penetration field  $H^*$  [8]. All the curves have been obtained with  $T = T_c/4$  and  $\lambda_0/\delta_0 = 10^{-2}$ ; furthermore, for simplicity, it was supposed  $H_{c1} = 0$ . It is evident that, taking into account the distribution of

$B$ , different field dependencies of  $R_s$  arise. In particular, a comparison between curves (b) and (c) shows that the greater  $H^*$ , the lower the value of  $R_s$ ; this is a consequence of the fact that the induction field of the whole sample decreases on increasing  $H^*$ . Another important characteristic of the  $R_s(H_0)$  curves is the change of concavity occurring at  $H_0 = H^*$ . When the fluxon lattice moves in the flux-flow regime and  $B$  is uniform, it is expected  $R_s \propto \sqrt{B}$ , with  $B \approx \mu_0 H_0$ , which leads to a negative concavity of the  $R_s(H_0)$  curve. For the general case of spatially-dependent flux density, the concavity of the  $R_s(H_0)$  curve is determined by the external-field dependence of  $B$ . The change of concavity of the curves (b) and (c) of Fig. 2, occurring at  $H_0 = H^*$ , can be qualitatively explained recalling that, for the critical state à la Bean, the induction field of the sample depends quadratically on  $H_0$  for  $H_0 < H^*$  and linearly on  $H_0$  for  $H_0 \geq H^*$  [8].

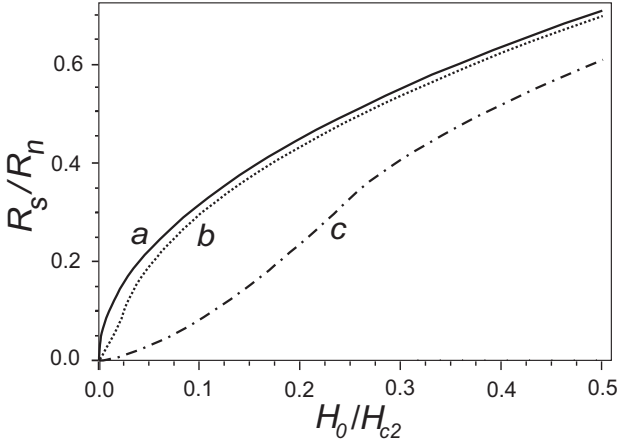


FIG. 2: Normalized  $R_s(H_0)$  curves, expected in the flux-flow regime, in the different cases: (a)  $B$  uniform; (b) critical state à la Bean with  $H^* = H_{c2}/40$  and (c)  $H^* = H_{c2}/4$ .  $T = T_c/4$ ,  $\lambda_0/\delta_0 = 10^{-2}$ .

When the field dependence of the critical current is taken into account,  $R_s$  strongly depends on the  $B$  profile due to the specific  $J_c(B)$  behavior. The field dependence of  $J_c$  has been widely discussed in the literature both theoretically [9, 14, 15] and experimentally [16, 17, 18]; different behaviors have been suggested. In Fig. 3 we report the expected  $R_s(H_0)$  curves, obtained considering different  $J_c(B)$  laws, along with the curve expected from the CC theory (a); also in this case, we have assumed  $H_{c1} = 0$ . Curve (b) has been obtained using  $J_c = J_0 \exp(-B/\Gamma_0)$ , curve (c) with  $J_c = J_0 - \alpha B$  and curve (d) with  $J_c = J_0$ ; the inset shows the corresponding  $J_c(B)$  laws used. As one can see, the features of the  $R_s(H_0)$  curve strongly depend on the profile of  $B$  inside the sample. In particular, looking at curve (b), it is evident that when the critical current verges on zero the  $R_s(H_0)$  curve approaches the one obtained from the CC theory, as expected. This finding is expected, in any case, for magnetic fields close to  $H_{c2}(T)$ , where the pin-

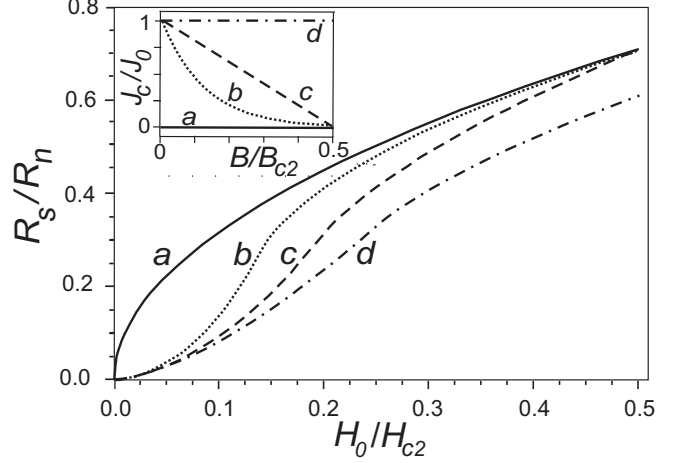


FIG. 3: Expected  $R_s(H_0)$  curves, obtained using for the field dependence of the critical current density the laws shown in the inset.  $T = T_c/4$ ,  $\lambda_0/\delta_0 = 10^{-2}$ .

ning becomes ineffective and, consequently,  $J_c \approx 0$ .

In order to study the peculiarities of the  $R_s(H_0)$  curve in superconductors in the critical state, we have measured the field-induced variations of  $R_s$  in bulk Nb at low temperatures, where the pinning effects should be significant. The sample, of dimensions  $3.3 \times 2.3 \times 1.3$  mm<sup>3</sup>, has been cut from a Tokyo Denkai batch with RRR = 300 and undergoes a superconducting transition at  $T_c \approx 9.2$  K. We have studied the Nb because the depinning frequency [21] is small enough to suppose that the mw current induces the fluxon lattice moving in the flux-flow regime; furthermore, our experimental apparatus allows reaching dc magnetic fields of the order of  $H_{c2}$ .

The mw surface resistance has been measured using the cavity-perturbation technique [19]. A copper cavity, of cylindrical shape with golden-plated walls, is tuned in the TE<sub>011</sub> mode, resonating at 9.6 GHz. The cavity is placed between the poles of an electromagnet, which generates magnetic fields up to  $\approx 1$  T. The sample is located in the center of the cavity where the mw magnetic field is maximum. The field geometry is that shown in Fig. 1 (b) and, therefore, the mw current induces a tilt motion of the whole fluxon lattice. The  $R_s$  values are determined measuring the variation of the quality factor of the cavity, induced by the sample, by means of an hp-8719D Network Analyzer.

Fig. 4 shows the field-induced variations of  $R_s$ , obtained in the Nb sample at the two temperatures  $T = 4.2$  K (a) and  $T = 2.2$  K (b).  $\Delta R_s(H_0, T) \equiv R_s(H_0, T) - R_{res}$ , where  $R_{res}$  is the residual mw surface resistance at  $T = 2.2$  K and  $H_0 = 0$ ; the data are normalized to the maximum variation,  $\Delta R_s^{max} \equiv R_n - R_{res}$ . The dashed and pointed lines are the curves expected from the CC model; the continuous lines are those obtained in the framework of our model; all the expected curves are plotted for  $H_0 > H_{c1}$ . The essential parameters to

calculate the expected curves are:  $\lambda_0/\delta_0$ ,  $H_{c2}(T)$  and the  $J_c(B)$  law. According to the results reported in the literature [22, 23], we have used  $\lambda_0/\delta_0 = 3 \times 10^{-2}$ ; however, for  $T < T_c/2$  the expected results are little sensitive to variations of this parameter.  $H_{c2}(4.2 \text{ K})$  has been determined experimentally and it results 1.1 T; the value of the upper critical field at  $T = 2.2 \text{ K}$  has been used as fitting parameter and we have found  $H_{c2}(2.2 \text{ K}) = 1.8 \text{ T}$ . To take into account the presence of the critical state, we have used a field dependence of  $J_c$  similar to that reported by Cline *et al.* [20] for Nb crystals; in particular, it has been used a linear field dependence of  $J_c$  at low fields, followed by an exponential decrease for  $H_0 \geq H'$ . The value of  $H'$  has been considered as fitting parameter; the best-fit curves (continuous lines of Fig. 4) have been obtained using  $H'(4.2 \text{ K}) = 0.35 \text{ T}$  and  $H'(2.2 \text{ K}) = 0.5 \text{ T}$ . The  $B$  profiles, obtained on increasing  $H_0$ , which come out from the used  $J_c(B)$  laws, are shown in the insets.

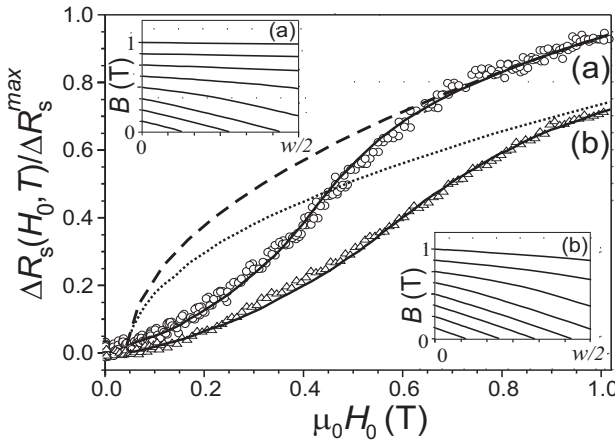


FIG. 4: Normalized field-induced variations of  $R_s$  at:  $T = 4.2 \text{ K}$  (a) and  $T = 2.2 \text{ K}$  (b). Symbols are the experimental results. Dashed and pointed lines have been obtained from the CC model using  $\lambda_0/\delta_0 = 3 \times 10^{-2}$ ;  $H_{c2}(2.2 \text{ K}) = 1.8 \text{ T}$  and  $H_{c2}(4.2 \text{ K}) = 1.1 \text{ T}$ . The continuous lines are the best-fit curves of the data, obtained using the same values of  $\lambda_0/\delta_0$  and  $H_{c2}(T)$  and the  $B$  profiles shown in the insets.

As one can see, in the whole range of  $H_0$  investigated the experimental results are quite well accounted for by considering the  $B$  distribution inside the sample. At low fields, the non-uniform  $B$  profile affects to a detectable extent the energy losses, giving rise to the positive concavity of the  $R_s(H_0)$  curve. On increasing  $H_0$ , the critical current, and consequently the slope of the field profile, decreases; the critical-state effects become less and less important and, eventually, when  $H_0$  approaches  $H_{c2}(T)$ , the observed behavior of  $R_s(H_0)$  is consistent with that expected from the CC model.

In summary, we have studied the field-induced energy losses in superconductors in the critical state. We have shown that the distribution of the local vortex magnetic

field in the sample can strongly affect the field dependence of the mw surface resistance. The analysis has been carried out for the field geometry in which the mw current induces a tilt motion of the fluxon lattice; indeed, in this case, the non-uniform flux distribution most affects the  $R_s(H_0)$  curve. The expected curves have been obtained supposing that the fluxons move in the flux-flow regime, where the field-induced energy losses are relevant even for applied fields much smaller than  $H_{c2}$ ; on the other hand, the analysis can be easily extended to a more general case, provided that the field dependence of the depinning frequency is known. We have highlighted that the effects of the critical state on the mw energy losses cannot generally be disregarded to account for the experimental data. Experimental results of field-induced variations of  $R_s$  in a Nb bulk sample at low temperatures have been justified quite well in the framework of our model.

We thank G. Lapis and G. Napoli for technical support.

---

- [1] J. I. Gittleman and B. Rosenblum, Phys. Rev. Lett. **16**, 734 (1966).
- [2] M. Golosovsky, M. Tsindlekht, and D. Davidov, Supercond. Sci. Technol. **9**, 1 (1996) and Refs. therein.
- [3] J. Owliaei, S. Shridar, and J. Talvacchio, Phys. Rev. Lett. **69**, 3366 (1992).
- [4] S. Fricano *et al.*, Eur. Phys. J. B **41**, 313 (2004).
- [5] M. W. Coffey and J. R. Clem, Phys. Rev. Lett. **67**, 386 (1991); Phys. Rev. B **45**, 9872 (1992); **45**, 10527 (1992).
- [6] E. H. Brandt, Phys. Rev. Lett. **67**, 2219 (1991).
- [7] A. Agliolo Gallitto *et al.*, Phys. Rev. B **56**, 5140 (1997).
- [8] C. P. Bean, Phys. Rev. Lett. **8**, 250 (1962).
- [9] Y. B. Kim, C. F. Hempstead, and A. R. Strnad, Phys. Rev. Lett. **9**, 306 (1962).
- [10] L. Ji, M. S. Rzchowski, N. Anand, and M. Tinkham, Phys. Rev. B **47**, 470 (1993).
- [11] Balam A. Willemse, J. S. Derov, and S. Sridhar, Phys. Rev. B **56**, 11989 (1997).
- [12] J. Bardeen and M. J. Stephen, Phys. Rev. **140**, A1197 (1965).
- [13] The analysis can be generalized by introducing the field dependence of the depinning frequency in  $\tilde{\delta}_v(\omega, B, T)$ .
- [14] F. Irie and K. Yamafuji, J. Phys. Soc. Jpn. **23**, 255 (1967).
- [15] Ming Xu, Donglu Shi, and Ronald F. Fox, Phys. Rev. B **42**, 10773 (1990).
- [16] T. Kobayashi *et al.*, Physica C **254**, 213 (1995).
- [17] W. DeSorbo, Phys. Rev. **134**, A1119 (1964).
- [18] M. Dhallé *et al.*, Physica C **363**, 155 (2001).
- [19] M. R. Trunin, Physics-Uspekhi **41**, 843 (1998).
- [20] H. E. Cline, C. S. Tedmon, Jr., and R. M. Rose, Phys. Rev. **137**, A1767 (1965).
- [21] M. Golosovsky, M. Tsindlekht, H. Chayet, and D. Davidov, Phys. Rev. B **50**, 470 (1994).
- [22] A. A. Golubov *et al.*, J. Phys. I France **6**, 2275 (1996).
- [23] H. Padamsee, Supercond. Sci. Technol. **14**, R28 (2001).